Boosting near-UV and deep-UV performance of light-emitting diodes

Mike Cooke reports on recent research to improve photon extraction and material quality in deep-ultraviolet light-emitting diodes.

Although ultraviolet (UV) is not visible, it has many uses, and light-emitting diodes (LEDs) producing such light from 'near' ultraviolet (400–300nm) to 'deep' ultraviolet (300–200nm) wavelengths are the subjects of much research.

UV-LEDs are seen as being useful for spectroscopy, photopolymer curing, water/air purification, medical and biological disinfection, biochemical detection, non-line-of-sight communication, and special lighting. Also, some schemes for white light using phosphors are powered by near-UV in LED or laser diode systems.

Some of these applications need deep ultraviolet (DUV) wavelengths. In the DUV range, competing mercury-lamp systems have drawbacks such as fragility and bulk, along with short lifetime and low efficiency. And, of course, mercury is highly toxic. Shorter wavelengths are more effective in damaging or killing biological systems — for example, ~250nm is needed to break up DNA.

As wavelengths push into the DUV 200–300nm wavelength range, efficiency becomes particularly low, of the order a few percent. Sapphire is the preferred substrate, but suffers from lattice mismatch and thermal expansion mismatch with the active light-emitting aluminium gallium nitride (AlGaN) semiconductor material that introduces strain/stress, generating efficiency-killing defects.

Here we look at recent reports attempting to improve the performance of near-UV and deep-UV LEDs.

Reflecting on chromium/aluminium n-electrode

Researchers in China have been applying reflective n-type electrode metal structures to boost light extraction in 280nm-wavelength DUV-LEDs [Yang Gao et al, IEEE Transactions on Electron Devices, published online 21 May 2019].

The work by Huazhong University of Science and Technology and University of Science and Technology of China used a chromium/aluminium (Cr/Al) combination to enhance reflection of the electrodes on the n-type AlGaN contact layer of the LEDs. While the chromium absorbs DUV radiation, aluminium is highly reflective.

The researchers explain the need for chromium in the electrode: "If we only adopt the Al layer as the n-type electrode, it is almost impossible to form an ohmic contact with the Al-rich n-AlGaN. Therefore, a Cr metal layer must be introduced before the deposition of the

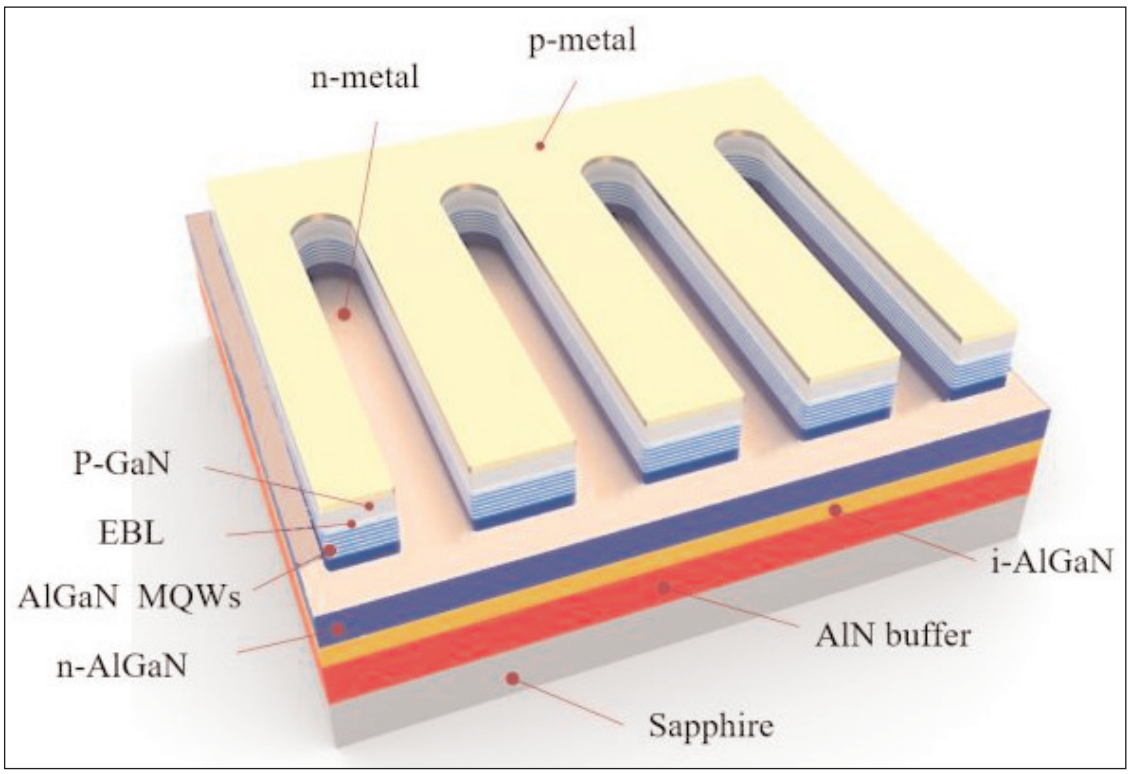

Figure 1. Schematic of flip-chip DUV-LED device.

Al layer to form an ohmic contact and improve the electrical performance."

The DUV-LED material was grown by metal-organic chemical vapor deposition (MOCVD) on c-plane sapphire. The buffer consisted of 2μm AlN. Undoped $Al_{0.55}Ga_{0.45}N$ was used for strain release before a silicon-doped n-$Al_{0.55}Ga_{0.45}N$ contact layer. The light-emitting active region contained five 2.5nm $Al_{0.37}Ga_{0.63}N$ quantum wells separated by 12.5nm $Al_{0.51}Ga_{0.49}N$ barriers. The p-side of the device consisted of magnesium-doped p-$Al_{0.7}Ga_{0.3}N$ and p-GaN contact layers.

The fabrication process was designed to create flip-chips with the DUV light emerging mainly through the sapphire substrate, since the bandgap of p-GaN is less than that of photon energy (Figure 1). The relatively narrow p-GaN gap makes it highly absorbing of the DUV. Unfortunately, magnesium doping of high-Al-content AlGaN results in very low enhancement of the hole concentration at room temperature due to a high activation energy.

DUV-LED fabrication began with inductively coupled plasma etch to expose the n-AlGaN contact layer.

The full scheme for the n-electrode consisted of chromium/aluminium/titanium/gold (Cr/Al/Ti/Au) deposited by electron-beam evaporation. The thicknesses of the Al, Ti and Au layers were 120nm, 40nm and 60nm, respectively. The chromium thickness varied from 1nm to 20nm. The n-electrode was annealed at 850ºC for 30 seconds in nitrogen.

The p-electrode consisted of nickel/gold/nickel/gold (Ni/Au/Ni/Au).

An LED with 2.5nm chromium in the n-contact had the lowest turn-on voltage of 4.7V (LED-2). The same device also had the lowest contact resistance. The ideality factor of the devices was similar, around 5.31.

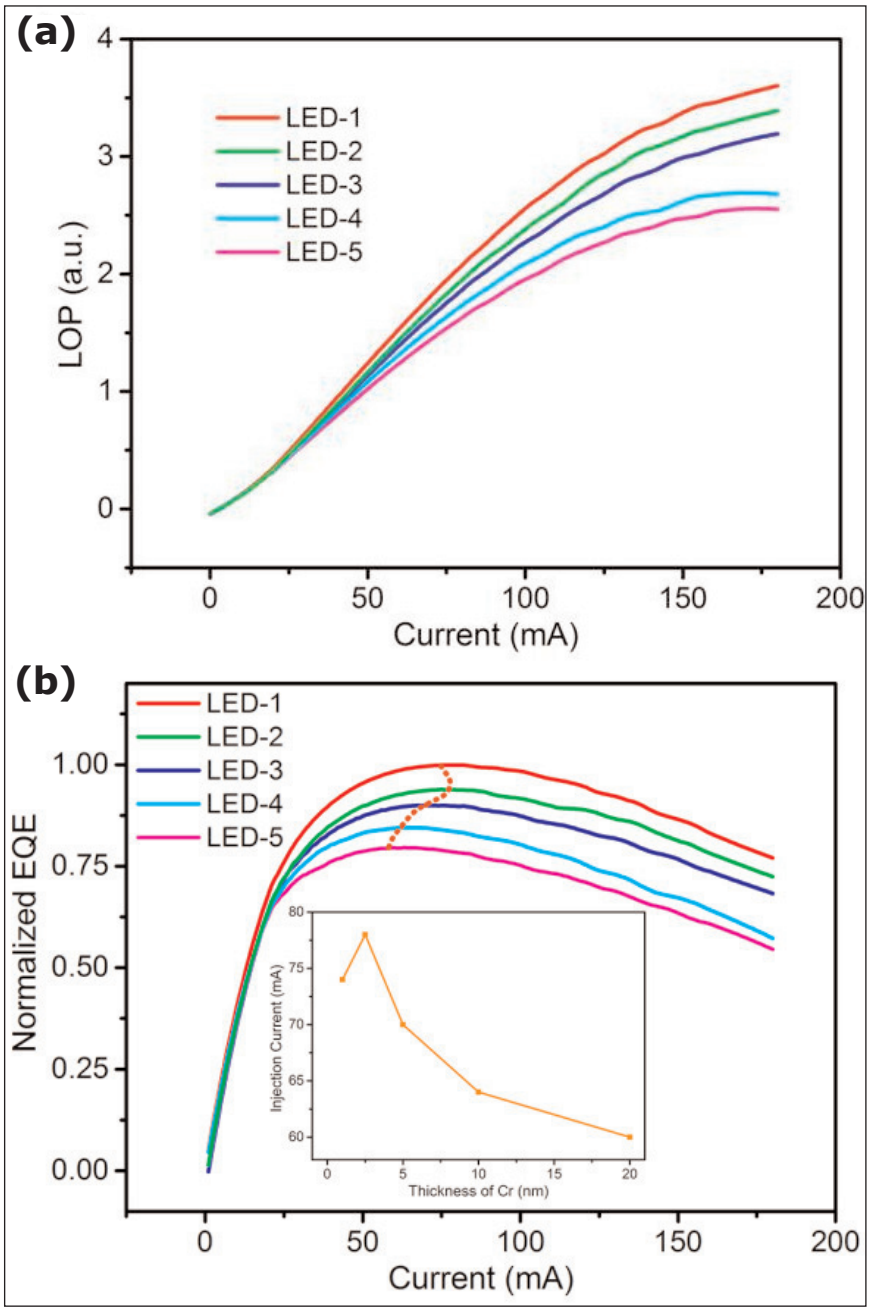

Figure 2. (a) LOP versus injected current for five fabricated DUV-LED devices. (b) EQE in terms of current. Inset: corresponding injection current to achieve peak EQE. LED-3 and LED-4 had 5nm and 10nm Cr, respectively.

In terms of light output power (LOP) at given current injection, the device with 1nm chromium in the reflector (LED-1) gave the highest value (Figure 2). At 180mA injection, the output power was 40.9% higher than that for the LED with the thickest chromium layer – LED-5 with 20nm Cr.

The researchers suggest that the higher turn-on voltage and contact resistance of LED-1 versus LED-2 could be due to the chromium layer being too thin to form the high-quality Al-Cr and Cr-N alloys needed for ohmic contact. The higher light output is attributed to the high reflectivity of the Al layer.

The peak external quantum efficiency (EQE) for LED-1 was 25.4% greater than that of LED-5. The corresponding figure for LED-2 was 17.9%. The current injection point of the peak efficiency varied with device: 74mA for LED-1, 78mA for LED-2, and 60mA for LED-5. The researchers explain the higher current injection for LED-2 as being due to its superior ohmic contact and electrical behavior. "Normally, a lower contact resistance or better ohmic contact can definitely improve current spreading and thus higher current injection efficiency," the team writes.

The reflectivity of Cr/Al metal stacks on sapphire was measured at 280nm center wavelength and compared with results from an unalloyed Al layer. The relative reflection was 93.1% for 1nm and 82.2% for 2.5nm Cr.

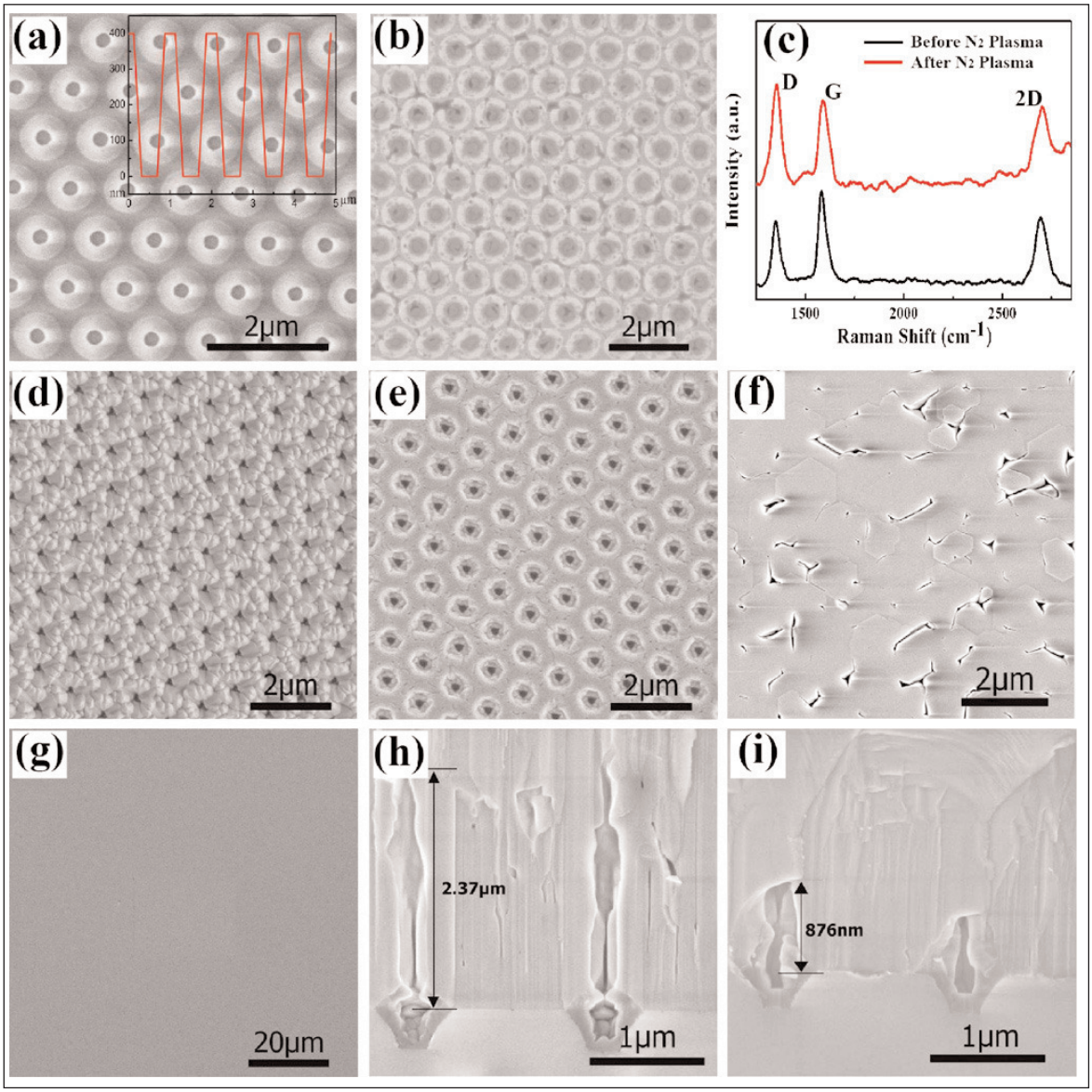

Figure 3. (a) SEM image of bare NPSS. Inset in (a) shows line profile from atomic force microscopy. (b) SEM image of as-grown graphene films on NPSS. (c) Raman spectra of graphene film before (black) and after (red) nitrogen plasma treatment. (d) and (f) SEM images of initial 10 minutes and 2 hours growth of AlN films on NPSS without graphene interlayer. (e) and (g) SEM images of initial 10 minutes and 2 hours growth of AlN films on NPSS with graphene interlayer. (h) and (i) Cross-sectional SEM images of AlN films on NPSS without and with graphene interlayer.

Graphene on nano-patterned sapphire

Researchers in Beijing, China, have used graphene (Gr) to improve AlN growth on nano-patterned sapphire substrates (NPSSs) as a template for AlGaN DUV LEDs [Hongliang Chang et al, Appl. Phys. Lett., vol114, p091107, 2019].

The team was variously based at Research and Development Center for Semiconductor Lighting Technology, University of Chinese Academy of Sciences, Peking University, and State Key Laboratory of Superlattices and Microstructures.

The presence of graphene improved aluminium mobility on the growth surface, improving crystal quality through quasi-van der Waals epitaxy (QvdWE). In turn, this improved the performance of an AlGaN LED grown on the AlN template.

The NPSS consisted of 400nm-deep nano-concave cone patterns with 1μm period produced by nano-imprint lithography on the sapphire surface. The unetched regions were 300nm wide. The ~0.7nm-thick graphene layer was grown by 1050ºC catalyst-free atmospheric pressure chemical vapor deposition (APCVD). The graphene growth process took three hours. The precursor was methane in hydrogen/argon carrier.

The graphene was subjected to reactive ion etch to introduce defects that would increase chemical reactivity with the subsequent AlN growth. Without defects, AlN does not attach easily to graphene, slowing AlN growth.

The graphene on NPSS was prepared with 30-second exposure to nitrogen plasma before loading into the metal-organic chemical vapor deposition reactor for AlN growth. Raman spectroscopy suggested that the nitrogen plasma treatment generated increased numbers of dangling bonds.

The 1200ºC AlN growth used trimethyl-aluminium and ammonia precursors in hydrogen carrier gas. There was no low-temperature nucleation step. The full growth time was two hours. Some samples were grown for just 10 minutes to allow study of the initiation of AlN deposition.

Without a graphene interlayer, two hours of growth on NPSS resulted in rough, non-uniform AlN layers (Figure 3). By contrast, the graphene interlayer

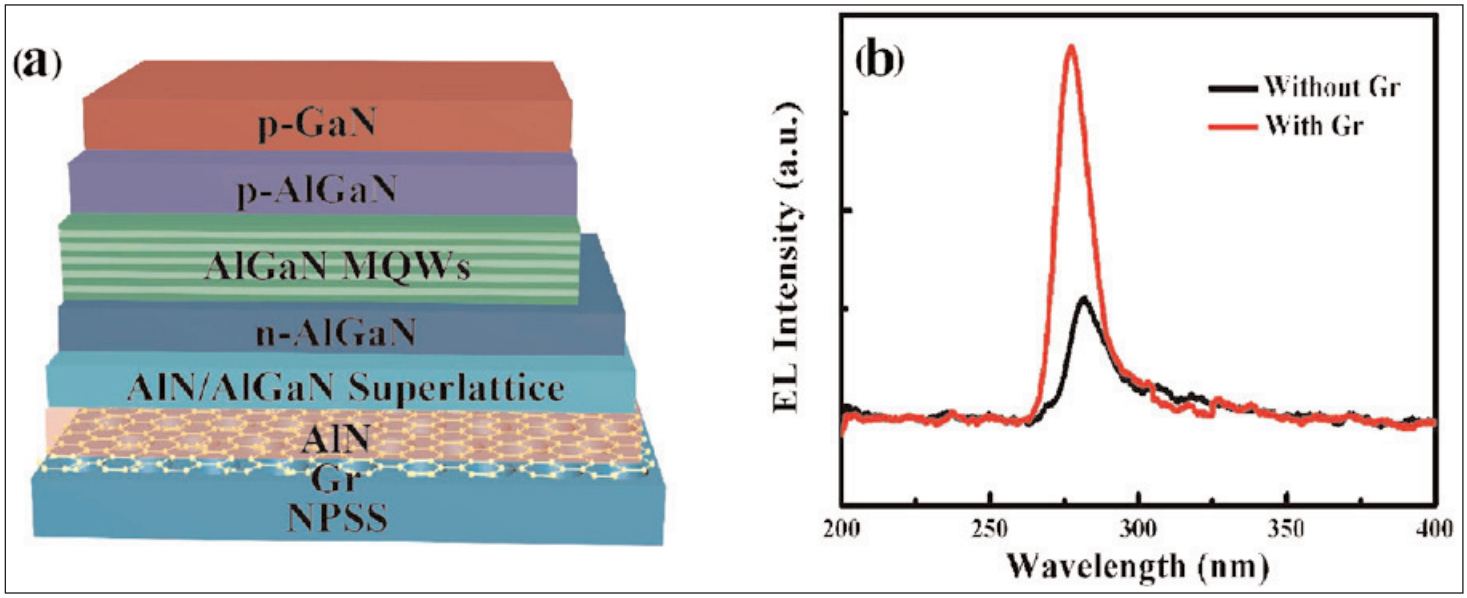

Figure 4. (a) Schematic of AlGaN-based DUV-LED. (b) Electroluminescence spectra with and without Gr interlayer.

enabled rapid coalescence of the AlN, giving a continuous, flat surface. Cross-sectional scanning electron microscopy (SEM) showed the coalescence occurred within 1μm of the full ~2.4μm growth.

X-ray rocking-curve analysis showed a reduction in the full-width at half maximum (FWHM) of the peak associated with the (0002) plane of the AlN lattice from 455.4arcsec to 267.2arcsec, arising from the graphene interlayer. The $(10\bar{1}2)$ peak FWHM also decreased from 689.2arcsec to 503.4arcsec. These values resulted in respective estimates for screw and edge dislocations: $4.51 \times 10^8/cm^2$ and $4.40 \times 10^9/cm^2$ without graphene interlayer, reducing to $1.55 \times 10^8/cm^2$ and $2.60 \times 10^9/cm^2$ with graphene.

According to Raman spectroscopy, the biaxial stress was reduced from 0.87GPa to 0.25GPa by the use of graphene interlayers.

Simulations of the growth process suggested that the effect of the graphene layer was to increase the mobility of aluminium adatoms, compared with the bare NPSS surface. The researchers comment: "The strong binding of Al adatoms to the defect sites and the free diffusion on the non-defective regions ensure the effective nucleation and fast growth for AlN layers, as observed in our experiments."

The AlN on bare NPSS undergoes "three-dimensional longitudinal island growth" due to the sluggish diffusion of the Al adatoms. The coalescence of the islands is therefore delayed. On graphene, the Al adatoms can diffuse further in shorter time, allowing "lateral two-dimensional growth" with rapid lateral coalescence.

The researchers used the AlN/Gr/NPSS template to produce a deep-ultraviolet LED (Figure 4). The epitaxial structure consisted of 1130ºC 20-period 2nm/2nm $AlN/Al_{0.6}Ga_{0.4}N$ superlattice, 1.8mm n-$Al_{0.55}Ga_{0.45}N$ contact, 5-period 3nm/12nm $Al_{0.4}Ga_{0.6}/Al_{0.5}Ga_{0.5}N$ multiple quantum well, 50nm p-$Al_{0.65}Ga_{0.35}N$ electron blocking layer, 30nm p-$Al_{0.5}Ga_{0.5}N$ cladding and 150nm p-GaN contact. Post-growth annealing was used to activate the p-type layers (800ºC for 20 minutes in nitrogen).

At 40mA, the 280nm-wavelength peak was around 2.6x higher than that for electroluminescence from an LED grown on bare NPSS. The researchers attribute the higher intensity to a reduced defect density in the Gr-based sample.

Shell/core nanowires

National Institute of Standards and Technology (NIST) and University of Colorado in the USA have reported AlGaN/GaN shell/core nanowire 365nm near-UV LEDs that demonstrated ~5x the light output compared with GaN/GaN nanowire devices [Matt D Brubaker et al, Nanotechnology, vol30, p234001, 2019].

Nanowire structures might also be useful in boosting the pitiful efficiencies in high-Al-content AlGaN DUV LEDs based on conventional technology.

First ordered arrays of nanowires were grown using plasma-assisted molecular beam epitaxy (PAMBE) on nitrogen-polar GaN/AlN templates on (111) silicon with a silicon nitride mask. The holes in the mask for nanowire growth were 80–240nm diameter with 300–10,000nm pitch. The silicon-doped n-GaN cores were grown at 860ºC substrate temperature. The core length was about 2μm. The ~40nm-thick silicon-doped $Al_{0.09}Ga_{0.91}N$ shell was grown at 700ºC.

Photoluminescence spectra measured at 5K suggested that the Al mole fraction of the shell tip decreased with nanowire diameter. By contrast, reducing the pitch increased Al concentration. The decrease in Al content at the nanowire tip was related to reduced mobility of the atoms at the growing tip, compared with Ga.

The Al content of the main shell of the nanowire stems was more difficult to determine, probably due to

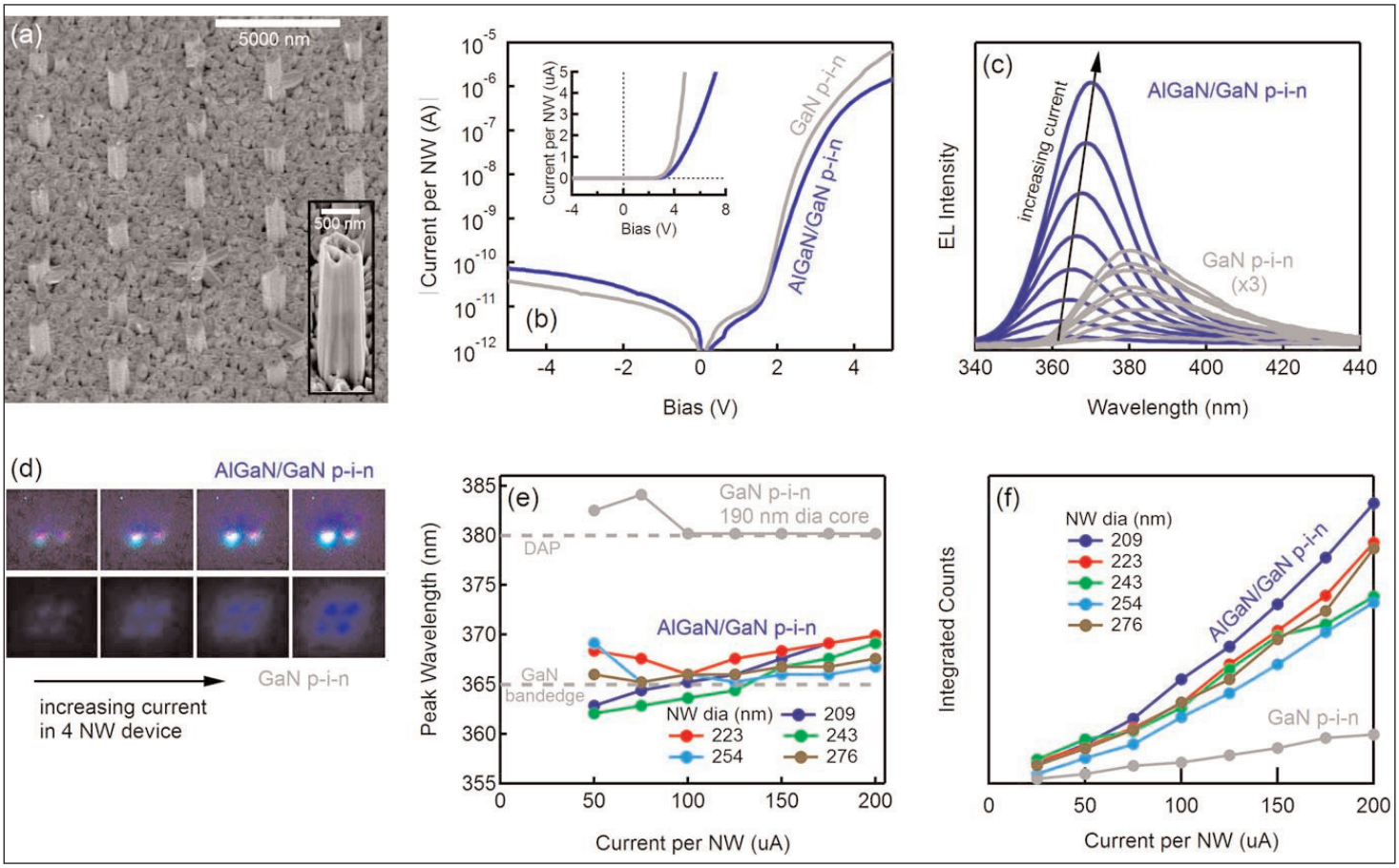

Figure 5. Core–shell p–i–n nanowire LED characteristics comparing AlGaN/GaN heterojunctions and GaN/GaN homojunctions. (a) Scanning electron micrograph of post-metallization AlGaN/GaN core–shell LEDs, with (inset) pre-metallization single nanowire. (b) Current-voltage characteristics and (c) EL spectra for 25 nanowire LEDs. (d) EL images for 4 nanowire LEDs are shown in the figure. GaN p–i–n EL intensities multiplied by factor of three. (e) Peak emission wavelength and (f) integrated intensity versus current for various core diameters.

non-radiative recombination, surface states and defects. The researchers used emissions from excitons (bound electron-hole states) to estimate Al content. Smaller-diameter nanowires were found to have higher-Al-content shells. Smaller-pitch arrays had low Al concentration.

The nanowire growth process was modified to include doping for p-i-n LEDs. The n-GaN core region was grown to a height of 3.3μm pitched at 5μm. Shell growth was initiated with 15nm n-GaN followed by ~85nm intrinsic AlGaN, ~285nm p-AlGaN, and ~5nm heavily doped p^{++}-AlGaN.

The LED p-contact electrode was constructed by 20nm/200nm Ni/Au deposition at normal incidence, followed by 200nm Au at 45º. This covered one side of the wires with metal while the other side allowed light extraction. The n-side current flow was through the buffer with electrical isolation provided by the silicon nitride nanowire growth mask.

The researchers compared the performance of the AlGaN/GaN heterojunction LEDs with GaN/GaN homojunction nanowire devices previously reported by the group (Figure 5). The turn-on voltage of the AlGaN/GaN LEDs was higher than that for GaN/GaN, "likely related to the reduced electron overflow current and increased barrier to hole injection expected for higher Al mole fractions," according to the team.

Subjecting the AlGaN/GaN LED to prolonged current injection seemed to have an electrical annealing effect on the p-contact, giving increased electroluminescence (EL) intensity and lower series resistance. The researchers comment: "Further development of optimized p-contact metallization and annealing processes are expected to reduce burn-in effects and improve overall device performance."

The EL from the AlGaN/GaN was around 365nm wavelength, close to the band edge of GaN. This was in contrast to the GaN/GaN LEDs, which emitted around 380nm, corresponding to donor-acceptor-pair (DAP) recombination from electrons injected into the p-GaN shell, according to the researchers. The team also suggests that GaN core emissions could be reabsorbed in the GaN shell, unlike with the wider-bandgap AlGaN.

The 380nm emission and 365nm reabsorption effects are stopped by the wider-bandgap AlGaN, which is also commonly used as an electron-blocking layer in standard GaN LEDs. The researchers report that the integrated EL intensity in the AlGaN/GaN nanowire LEDs

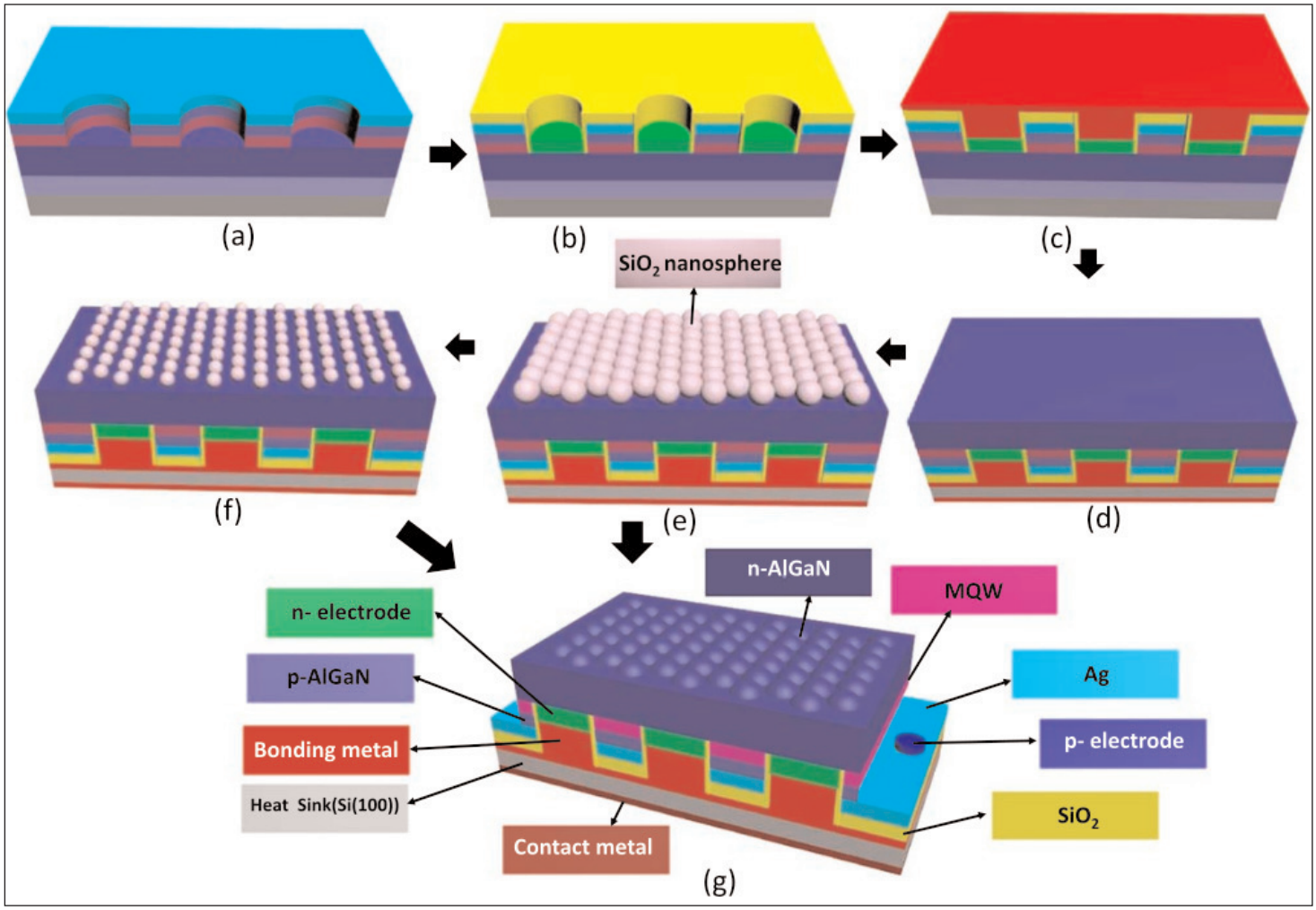

Figure 6. Schematic fabrication process: (a) deposition and patterning of silver-based reflective electrode with ICP etched vias for embedded n-contact to n-AlGaN layer; (b) deposition of Cr/Al n-type contact metal and silicon dioxide (SiO_2) insulating layer; (c) deposition of nickel/tin bonding metal and flipping onto silicon (100) wafer; (d) removal of silicon growth substrate and etch away AlGaN buffer layer, (e) SiO_2 nano-sphere single layer fabricated on N-face n-AlGaN, (f) tailored SiO_2 nanosphere on N-face n-AlGaN, (g) AlGaN nanostructure (nanorod, nano-trapezoid, nanodome and nanocone) arrays on UV LED chips.

was around 5x that of the GaN/GaN reference for a given current injection.

Thin-film surface nano-structuring

Researchers based in China have used thin-film and surface nanostructuring to boost the performance of ~370nm near-UV LEDs by a factor of 3.9 [Chuanfei Ma et al, Nanotechnology, vol30 p185201, 2019].

The nanostructuring was performed on the thick AlGaN n-side of the devices. This was enabled by flipping the LED material over onto another wafer and removing the silicon growth substrate. The nanostructuring was designed to reduce total internal reflection that traps light due to the large contrast in refractive index between III–nitride materials (~2.4) and air (1). The light emission was from indium gallium nitride (InGaN) multiple quantum wells (MQWs).

The team from Suzhou Institute of Nano-Tech and Nano-Bionics and University of Science and Technology of China grew the UV LED structure on silicon in the (111) crystal orientation. Metal-organic vapor phase epitaxy (MOVPE) deposited AlN/AlGaN as a multi-layer buffer, n-AlGaN cladding, an InGaN/AlGaN pre-strained superlattice, InGaN quantum wells in AlGaN barriers, p-AlGaN electron blocking, p-AlGaN current spreader and p-GaN contact.

The epitaxial material was processed into vertical thin-film LED chips (Figure 6). The structure included an embedded n-contact and a silver-based reflective p-electrode. The embedded n-contact clears the ultimate emission surface from blockage by contact electrodes and pads.

The nanostructuring of the nitrogen-face AlGaN was prepared with an oxygen-plasma treatment to convert the bonding from hydrophobic to hydrophilic for spin-coating of the SiO_2 nanospheres to create a self-assembled array. Fluorine-based reactive ion etch was used to 'tailor' the sphere sizes to enable subsequent chlorine-based inductively coupled plasma (ICP) etch of the AlGaN surface into 'nanodomes'. The nanospheres

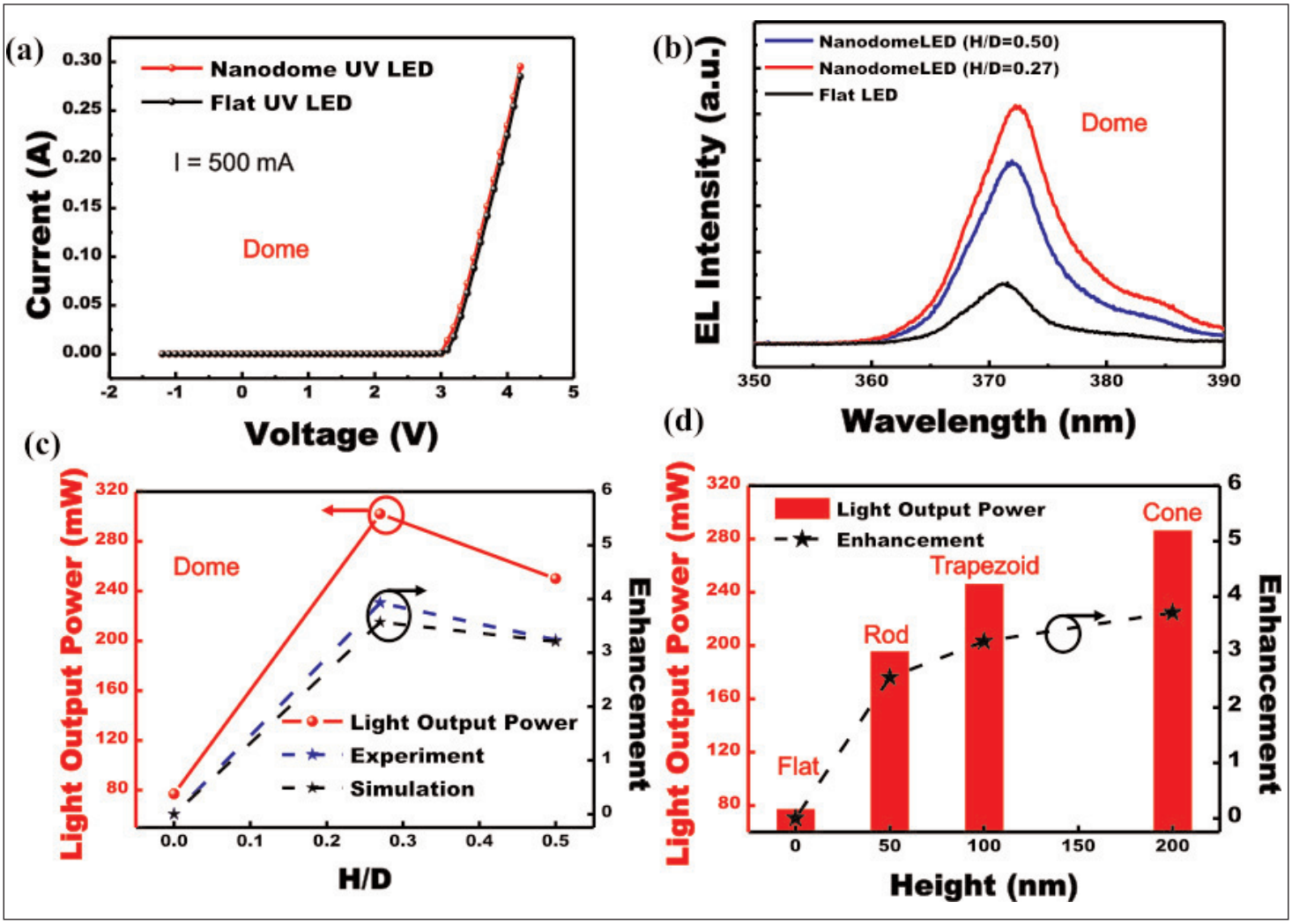

Figure 7. (a) Current-voltage curves of nanodome and flat UV LEDs, (b) electroluminescence spectra, (c) experimental and simulated light output power with various H/D nanodomes, (d) experimental light output power with nanorod, nano-trapezoid and nanocone arrays.

were removed with a buffered oxide etch and dry etch damage of the nanodomes was smoothed with hydrochloric acid treatment.

The group performed ray-tracing Monte Carlo simulations and chose 250nm-diameter SiO_2 nanospheres to create the domes. The simulations suggested an optimum height/diameter (H/D) ratio of 0.27, which gave a 68% light extraction efficiency, compared with 19% for a flat surface.

The current–voltage performance of LEDs with and without nanodomes was almost identical (Figure 7). The researchers point out that nanostructuring of the 2.5μm-thick n-AlGaN layer allows a large process window, in contrast to nanostructuring the thin ~100nm p-side of the device. Dry etching of the thin p-side layer carries risks of reducing conductivity, current spreading, etc. Further, such processing can also affect the underlying MQWs, reducing the efficiency of photon emission. Combined, one expects adverse effects on electrical and light-emission performance.

The integrated electroluminescence of the nanodome LEDs with 0.27 H/D ratio achieved 3.9x the performance of flat reference devices. Simulations suggested a 3.6x boost. The researchers also compared the performance of flat LEDs, against devices with 'rod', 'trapezoid' and 'cone' nanodome structures. The structures were achieved by not reducing the 250μm-diameter nanospheres with reactive ion etch and just performing the inductively coupled etch for different process times.

The researcher also examined the far-field radiation pattern and found that nanodomes cast the emissions more in the forward direction, compared with the flat LEDs. The researchers comment: "This phenomenon was more pronounced for the nanodome structure with H/D = 0.5, indicating that the nanostructures would facilitate the light extraction along the vertical direction, which is particularly useful to UV curing and other related applications of UV LEDs."

The team adds that the AlGaN nanostructuring technique could be easily extended to deep UV vertical LEDs for enhancing light extraction. ■

The author Mike Cooke has worked as a semiconductor and advanced technology journalist since 1997.